

## Effect of mono- and multi-valent ionic environments on the in-lattice nanoparticle-grafted single-stranded DNA

Sunita Srivastava,<sup>1\*</sup> Anuj Chhabra<sup>2</sup> and Oleg Gang<sup>3,4,5\*</sup>

<sup>1</sup>Department of Physics, Indian Institute of Technology Bombay, Mumbai, 400076, India

<sup>2</sup>Center for Nanoscience, Indian Institute of Technology Bombay, Mumbai, 400076, India

<sup>3</sup>Center for Functional Nanomaterials Brookhaven National Laboratory Upton, NY 11973, USA

<sup>4</sup>Department of Chemical Engineering Columbia University New York, NY 10027, USA

<sup>5</sup>Department of Applied Physics and Applied Mathematics Columbia University New York, NY 10027, USA

*Table S1: The DNA sequence design (5' to 3') for systems presented in the paper. HSC6H12 represents the thiol modification. Sys A, Sys B, and Sys C have 30, 50, and 65 bases, respectively. Outer 15 bases are designed to form the Watson Crick Base pairing to form a self-assemble structure.*

DNA-AuNp System	Number of chains	DNA Sequence
Sys A	30	HSC6H12-TTTTTCGTTGGCTGTAACTAACCTTCAT
Sys A'	30	HSC6H12-TTTTTCGTTGGCTGTATGAAGGTTAGGTAA
Sys B	50	HSC6H12- TTTTTTTTTTTTTCGTTGGCTGGATAGCTGTGTTCTTAA CCTAACCTTCAT
Sys B'	50	HSC6H12- TTTTTTTTTTTTTCGTTGGCTGGATAGCTGTGTTCTATG AAGGTTAGGTAA
Sys C	65	HSC6H12- TTTTTTTTTTTTTTTTTTTTTTTTTTTTTTTTTCGTTGGCTGGATA GCTGTGTTCTTAACTAACCTTCAT
Sys C'	65	HSC6H12- TTTTTTTTTTTTTTTTTTTTTTTTTTTTTTTTTCGTTGGCTGGATA GCTGTGTTCTATGAAGGTTAGGTAA

## I. Small Angle X-ray Scattering for monovalent salt :

Small Angle X-ray Scattering has been used to understand the in-situ structural morphology of the DNA chains. Samples with DNA-AuNP superlattice aggregates were formed and transferred to the quartz capillary at varying monovalent salt concentrations. Capillaries were sealed to avoid any concentration change in the solvent to avoid any error in the measurement. Structure factor was calculated using the equation:  $S(q) = I(q)/F(q)$ , where  $I(q)$  is the calculated intensity for the DNA-AuNP superlattice and  $F(q)$  is the form factor. Fig. S1 shows the calculated structure factor for the DNA-AuNP at different salt concentrations for monovalent salt for Sys B. From  $S(q)$ , we observe that peaks are in the ratio of  $1, \sqrt{2}, \sqrt{3}, 2, \sqrt{5}$ , and so on, indicates the formation of assembly with a long-range order, where NPs are arranged in a closed packed body-centered cubic (BCC) lattice. Figure S1 shows that the structure factor peak moves towards higher  $q$  as the salt concentration increases, leading to the decrease in the superlattice size, thus decreasing the DNA chain length. A detailed analysis has been done to understand the effect of monovalent salt on the DNA chain morphology and discussed in the main text.

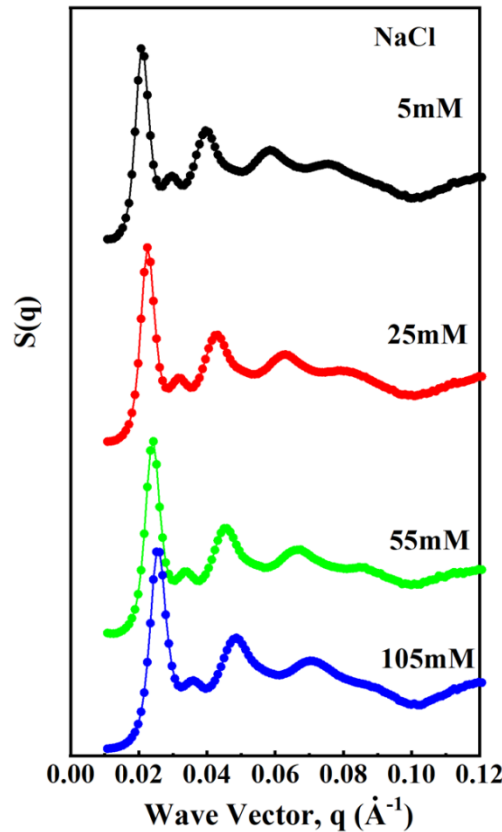


Fig. S1: Structure factor vs. wave vector, for Sys B with increasing concentration of added monovalent salt. The shift in the first diffraction peak towards the high wave vector indicates lattice shrinkage with added salt.

## II. Effect of the number of monomers:

Fig. S2 shows the effect on the increase of the number of monomers for a constant salt concentration. Power law analysis has been done to understand the effect of the number of monomers on the brush height for constant ionic strength. Brush length ( $H$ ) with the increase of the number of monomers can be approximated as  $H \sim N^\beta$ . For polyelectrolytes in a good solvent, the  $\beta$  value is theoretically found to be 0.6 [1, 2]. For monovalent salt, the average  $\beta$  is 0.556, and for divalent salt, this value is found to be 0.665. From this, it can be assumed that DNA chains attached to the spherical gold nanoparticles are in a good solvent.

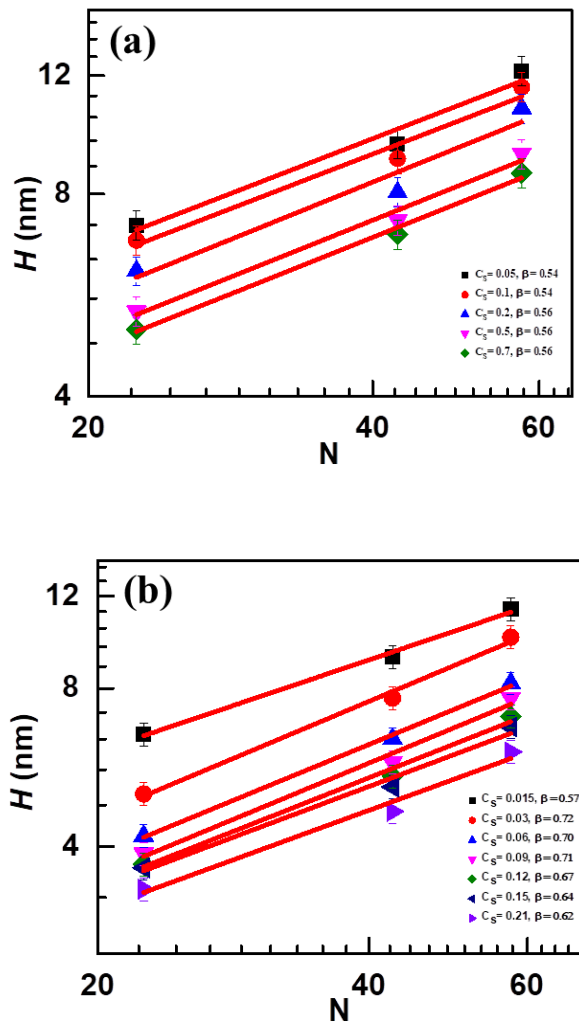


Fig. S2: Variation of  $H$  with the change in the number of monomers of the DNA chain can be approximated by  $H \sim N^\beta$ . a) shows the variation of  $H$  with the number of monomers of the DNA for constant ionic strength ( $C_s$ ) of the monovalent salt. b) Shows the variation of  $H$  with the number of monomers of the DNA for constant ionic strength ( $C_s$ ) of the divalent salt.

### III. Fitting data using planar brush model:

To understand the effect of the salt valency on the DNA chains attached on the gold nanoparticles, experimental data was fitted with the planar brush model given by the equation:

$$H \sim kNa(\sigma)^{1/3} C_s^{-\alpha}.$$

Here,  $N$ , is the number of monomers,  $a$  is the monomer size and  $\sigma$  is grafting density. In case of planar brush, the expected value of  $\alpha \sim 0.33$ , as reported in various systems experimentally[3] and theoretically[4].

We tried to fit our data with the above model for planar brush using the known estimates of  $N$  and  $\sigma$ . As it is evident from the Figure S3 planar brush model is unable to capture our data. If the fit is performed by varying  $\alpha$ , we get an estimate of  $\alpha \sim 0.13$ , which does not agree with the predictions of the planar brush model.

This suggests that the planar brush model is not able to incorporate the features in our data obtained from bulk systems and hence the modified Daoud Cotton Model needs to be considered.

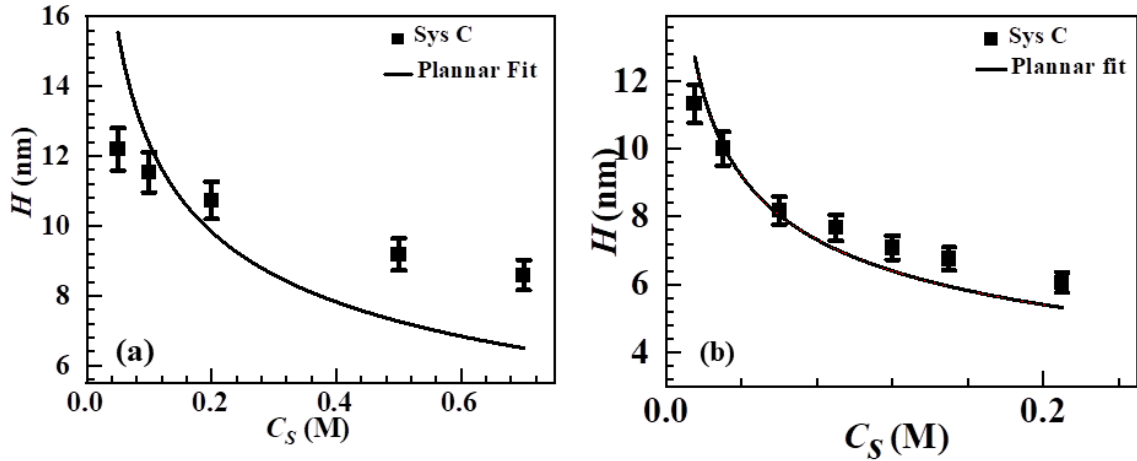


Fig. S3: The fit of the  $H(C_s)$  data using the planar brush model for system C in (a) monovalent salt (b) divalent salt environment.

### IV. Daoud Cotton model:

Daoud-Cotton[5] model described the structure of neutral star polymer as a function of a number of monomers, the number of chains in the star polymer, the size of the monomer, and excluded volume effects. But this model does not account for the size of a particle and

electrostatic interactions, relevant for our systems. To include the curvature effect and the effect of electrostatic interactions on the polyelectrolyte brush for a spherical surface, Zhulina et. al.[6] and Hariharan et. al.[7] modified the Daoud-Cotton model, and it is given by:

$$\frac{H}{R} + 1 = \left[ 1 + \frac{kNa}{R} \left( \frac{v\sigma}{l_k} \right)^{1/3} \right]^{3/5} \quad [1]$$

where  $R$  is the particle size,  $H$  is the brush length,  $k$  is the scaling constant,  $a$  is the size of the monomer,  $v$  is the excluded volume parameter,  $l_k$  is the Kuhn length,  $\sigma$  is the grafting density.

In Eq. 1, the electrostatic dependence of the excluded volume parameter,  $v$ , was not considered. However, we have found that excluded volume of PE chains depends in a complex manner on the salt ionic strength of the salt, and it's an important effect that needs to be considered explicitly. Also, Kuhn length is also dependent on the ionic strength and number of monomers in the chain. So this equation cannot be directly used to understand the effect of salt concentration and curvature effect on the DNA chains. This equation was further modified by Tan et. al.[8] which simplified the effect of excluded volume and Kuhn length. The modified version of the DCM is given by:

$$\frac{H}{R} + 1 = \left[ 1 + \frac{KNa}{R} \left( \sigma N^{-\beta_1} C_s^{-\alpha_1} \right)^{1/3} \right]^{3/5} \quad [2]$$

Where  $H$  is the brush height,  $K$  is the scaling factor,  $N$  is the number of monomers,  $C_s$  (M) is the ionic strength,  $\alpha_1$  is the scaling exponent related to ionic strength for the system,  $\beta_1$  is the scaling exponent related to the number of monomers,  $\sigma$  is the grafting density (chains/nm<sup>2</sup>),  $R$  (nm) is the radius of the spherical surface,  $a$  is the monomer size (nm).

Upon further simplification, equation [2] can be rewritten as:

$$\frac{H}{R} + 1 = \left[ 1 + \frac{C_s^{-\alpha_1/3} K N^{(3-\beta_1)/3} a}{R} (\sigma)^{1/3} \right]^{3/5} \quad [3]$$

where  $H$  is the brush length (nm),  $R$  is the radius of spherical surface (nm),  $K$  is the scaling constant is close to 1 and 0.5 for monovalent salt and divalent salt respectively,  $N$  is the number of monomer/bases,  $a$  is the monomer size (nm), and  $\sigma$  is the grafting density (nm<sup>-2</sup>) of the DNA chain on a nanoparticle surface.

Table S2: Parameters used to fit the modified Daoud Cotton model with the experimental data for good solvent conditions.

	<b>K (NaCl)</b>	<b><math>\alpha</math> (NaCl)</b>	<b>K (MgCl<sub>2</sub>)</b>	<b><math>\alpha</math> (MgCl<sub>2</sub>)</b>	<b><math>\beta</math></b>	<b>a (nm)</b>	<b><math>\sigma</math></b>
<b>Sys A</b>	1.15	0.57 $\pm$ 0.02	0.43	0.94 $\pm$ 0.073	0	0.64	0.2228
<b>Sys B</b>	0.92	0.47 $\pm$ 0.02	0.36	0.96 $\pm$ 0.03	0	0.64	0.2228
<b>Sys C</b>	0.87	0.63 $\pm$ 0.04	0.36	0.99 $\pm$ 0.04	0	0.64	0.2228

## V. Daoud Cotton model with poor solvent conditions:

We also analysed our data using Daoud-Cotton model, assuming that the chains are in poor solvent conditions. For such scenario, where the chain collapse the repulsive/poor interactions between solvent-polymer molecules can result in a scaling exponent  $\sim 1/3$ . Therefore, to test if this might be occurring, we fixed,  $\beta = 1/3$ , as per the poor solvent predictions and kept the  $N$ ,  $k$ , and  $\alpha$  as a variable. The nanoparticles radius,  $R$ , was fixed as per our estimates from TEM and SAXS measurements. We find that though we can fit the data, the estimates of  $N$  from such are much higher than expected based on the design, indicating that the assumption of poor solvent is not valid for our systems. The parameters obtained from the fit are summarized in Table S4. The shrinkage/collapse of DNA chains in our systems is due to screening of electrostatic interactions in case of monovalent salts and ion-bridging effect in case of divalent salt environment, but not due to the unfavorable interaction with solvent.

Table S3: Parameters from fit using poor solvent conditions for DNA chains in Daoud Cotton Model

<b>N</b>	<b><math>\alpha_1</math> (NaCl)</b>	<b><math>\alpha_1</math> (MgCl<sub>2</sub>)</b>	<b>Expected N</b>	<b>N (NaCl)</b>	<b>Error in N (NaCl)</b>	<b>N (MgCl<sub>2</sub>)</b>	<b>Error in N (MgCl<sub>2</sub>)</b>	<b>R</b>	<b><math>\beta_1</math></b>	<b><math>\sigma</math></b>
Sys A	0.52	0.90	22.5	117.8	423.5%	348.0	1446%	5	1.33	0.22
Sys B	0.50	0.95	42.5	349.32	721.8%	782.8	1614%	5	1.33	0.22
Sys C	0.51	0.94	57.5	1260.9	2091%	1519	2541%	5	1.33	0.22

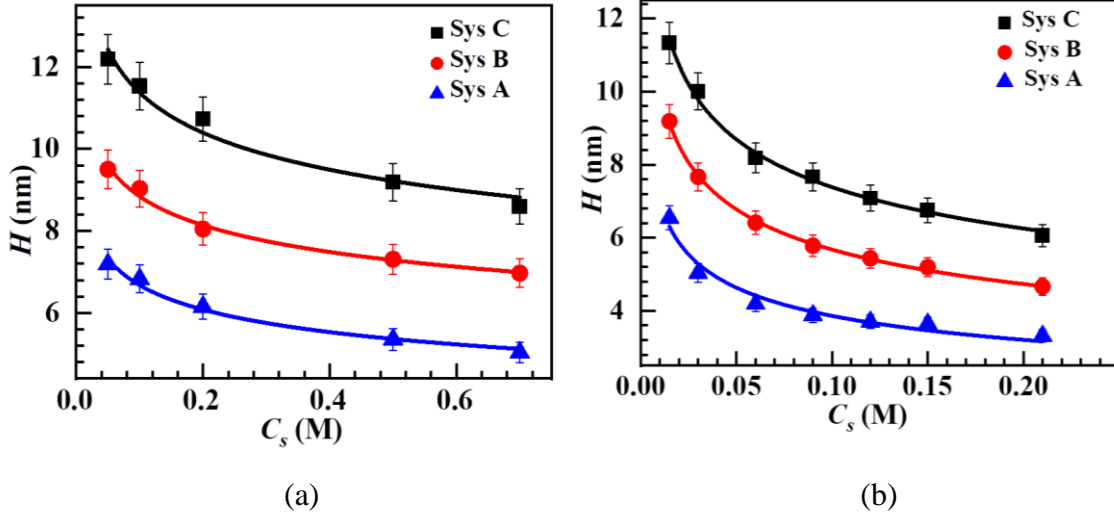


Fig. S4: Fit using modified Daoud-Cotton model, assuming poor solvent conditions as discussed above, for a) monovalent, b) divalent systems.

## VI. Daoud-Cotton model with multivariable fit:

To apply the Daoud-Cotton model we used a multivariable fit, where we fitted the experimental data for the monovalent salt system. In the first iteration we kept  $R$ , chain density and  $\beta_1$  constant and varied all other parameters including  $N$ ,  $k$ ,  $C_s$ ,  $\alpha_1$ . The results from the fit are summarized in Table 1. Note that the estimates of “ $N$ ” by fitting is closed to the known (based on the desing) value for system B and C. For system A, we find that the estimates of “ $N$ ” is off by  $\sim 83\%$ . We believe the large error in the estimates of  $N$  for system C may arise due to the approximation used for the estimate of  $H$ , where the chain conformations for double stranded parts are ignored. A system A (system with shorter chain length) has 33% of dsDNA whereas B and C has 17% and 13% respectively. As dsDNA has higher persistence length compared to ssDNA, this may contribute towards the higher value of  $N$  for the System A, as evident from the result of the fit.

Table S4: Parameters used to fit the experimental data with the modified Daoud-Cotton model while keeping  $R$ , grafting density and  $\beta_1$  constant.

<b>N</b>	<b>K</b>	$\alpha_1$	<b>N</b>	<b>Expected N</b>	<b>Error in N</b>	<b>R</b>	$\sigma$
Sys A	0.66	0.51	40.14	22.5	78.4%	5	0.22
Sys B	0.81	0.46	48.82	42.5	6.32	5	0.22
Sys C	0.94	0.57	56.5	57.5	1.7%	5	0.22

In the second iteration (Table 2) we kept chain density,  $K$  and  $\beta_1$  constant and varied all other parameters including  $R$ ,  $N$ ,  $k$ ,  $C_s$ ,  $\alpha_1$ .

*Table S5: Parameters used to fit the modified Daoud Cotton model with the experimental data by varying all the parameters except the grafting density and  $\beta_1$  and  $K$ .*

<b>N</b>	<b><math>\alpha_1</math></b>	<b>N</b>	<b>Expected N</b>	<b>Error in N</b>	<b>R</b>	<b>Error in R</b>	<b><math>\sigma</math></b>
Sys A	0.52	41.3	22.5	83.3%	3.9	21.2%	0.22
Sys B	0.46	48.3	42.5	12.0%	5.4	8.2%	0.22
Sys C	0.50	54.3	57.5	5.8%	6.7	33.4%	0.22

It was observed that parameters are dependent on each other, thus estimates of  $N$ ,  $\sigma$ ,  $\beta_1$ ,  $a$ , were fixed to fit the experimental data. These values were chosen as per the different systems as per the main text.

## **VII. Exponential Growth fitting of Fig 3 (main text)**

An exponential growth function can be defined by the equation:

$$\Delta H = H_{\text{NaCl}} - H_{\text{MgCl}_2} = A \cdot \exp(-C_s/t) + y_0 \quad [4]$$

Where  $y_0$  is the saturation value,  $H_{\text{NaCl}} - H_{\text{MgCl}_2}$  is the difference between the brush height for NaCl and brush height for MgCl<sub>2</sub>,  $t$  is the growth constant, and  $A$  is the fitting parameter  $y_0$  is the saturation value which depends upon the number of monomers. Parameters used to fit the equation are shown in Table S6. From the fitting parameters calculated from the above equation, we can calculate the saturation point. Saturation point can be observed as the ionic strength at which  $\Delta H$  value reaches is 99% of the  $y_0$ , i.e., for Sys A, Sys B, and Sys C. Ionic strength required to reach the final 99% of the  $\Delta H$  are  $\sim 0.07$ ,  $0.11$ , and  $0.16$  respectively.

For example, to calculate the saturation value for the Sys A, we use:

$$99\% \text{ of } y_0 (5.8) = -11.99 \cdot \exp(-C_{\text{sat}}/0.0139) + 5.8. \quad [5]$$

The estimates of different parameters obtained by fitting equation 4 to the experimental data is shown in Table S6. These values are used in equation 5 for estimation of saturation value  $C_s$ . The same procedure was done for Sys B and Sys C to calculate the saturation points.



Table S6: Parameters used to fit the difference between the brush height for NaCl and brush height for MgCl<sub>2</sub> with the exponential growth function.

System	A	Y0	t
Sys A	-11.99	5.8 ± 0.07	0.0137 ± 0.002
Sys B	-10.35	6.75 ± 0.04	0.0236 ± 0.001
Sys C	-9.77	8.94 ± 0.13	0.0343 ± 0.003

### VIII. Effect of trivalent salt:

Previously reported study in [9] show that the with increase of multivalent salt concentration, DNA, end to end distance first decreases but after a certain point, due to overcharging, it starts to increase. For divalent salt we do not observe the overcharging effect for our system. Since an overcharging is predominately observed in trivalent salts, we have performed experiments to unravel the effect of trivalent salts on the DNA-NP lattice structure in presence of trivalent salt environment ([Co(NH<sub>3</sub>)<sub>6</sub>]Cl<sub>3</sub>). The S(q) at varying ionic strengths of the added trivalent salt and correspondingly the estimates of the DNA brush length for system B for 15 nm AuNP are shown in Figure S5. For comparison we have plotted the estimates of DNA brush length in presence of all the three different salts and the data for trivalent salt is plotted separately on rescaled axis for a better clarity. It is evident from the data that there is no overcharging effects, as we did not observe any increase in DNA brush length. The estimates of  $H$  suggest that the DNA chain collapses at the low concentration of added trivalent salt ~2.4 mM. Thus, from our measurements of structural analysis using SAXS for trivalent salt, we conclude that DNA-NP systems do not depict overcharging effect for monovalent, divalent and trivalent salts.

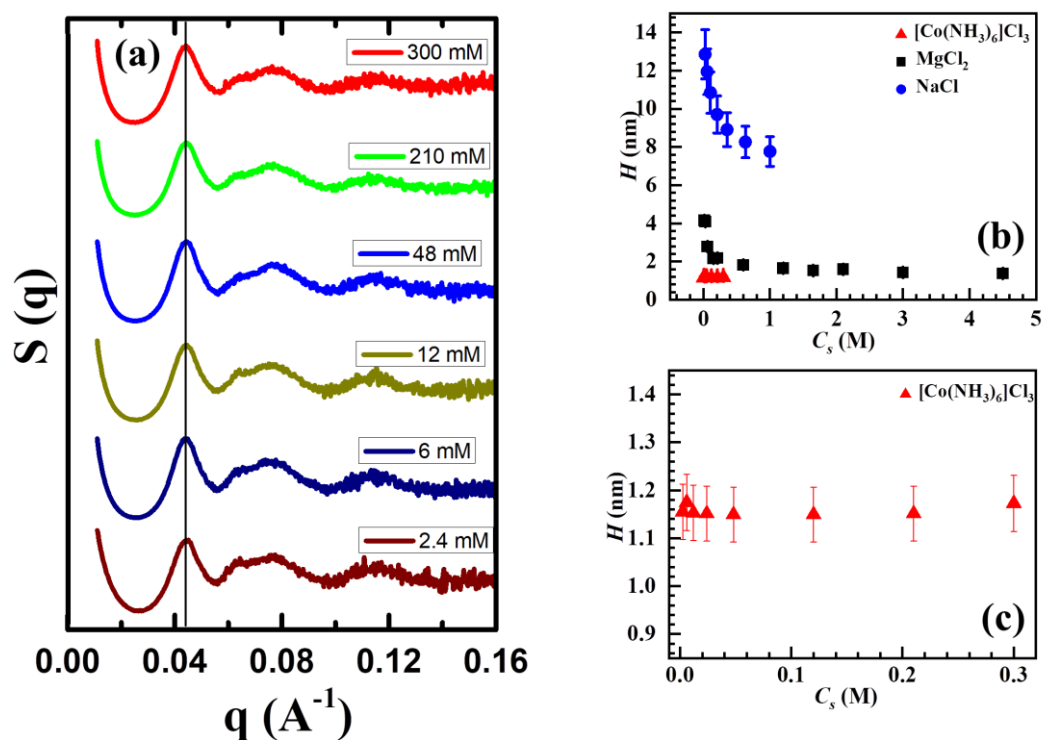


Fig. S5: a) Calculated structure factor in trivalent salt environment ( $[\text{Co}(\text{NH}_3)_6]\text{Cl}_3$ ), for 15 nm DNA-AuNP superlattice. With the increase of  $C_s$  we do not observe change in the peak position. b) Calculated brush length  $H$ , The  $H$  vs  $C_s$  for salt environment, as indicated in the legend. c) Brush length  $H$ , for DNA-AuNP superlattice with the increase of  $C_s$  of a trivalent salt.

## References:

1. Muthukumar, M., *Polymer translocation*. 2016: CRC press.
2. Rubinstein, M. and R.H. Colby, *Polymer physics*. Vol. 23. 2003: Oxford university press New York.
3. Yu, J., et al., *Structure of polyelectrolyte brushes in the presence of multivalent counterions*. 2016. **49**(15): p. 5609-5617.
4. Zhulina, E., O. Borisov, and T.J.M. Birshtein, *Polyelectrolyte brush interaction with multivalent ions*. 1999. **32**(24): p. 8189-8196.
5. Daoud, M. and J. Cotton, *Star shaped polymers: a model for the conformation and its concentration dependence*. Journal de Physique, 1982. **43**(3): p. 531-538.
6. Borisov, O., E.J.T.E.P.J.B.-C.M. Zhulina, and C. Systems, *Effects of ionic strength and charge annealing in star-branched polyelectrolytes*. 1998. **4**(2): p. 205-217.
7. Hariharan, R., et al., *Ionic Strength and Curvature Effects in Flat and Highly Curved Polyelectrolyte Brushes*. Macromolecules, 1998. **31**(21): p. 7506-7513.
8. Tan, S.J., et al., *Crystallization of DNA-Capped Gold Nanoparticles in High-Concentration, Divalent Salt Environments*. Angewandte Chemie International Edition, 2014. **53**(5): p. 1316-1319.
9. Wang, F.H., Y.Y. Wu, and Z.J. Tan, *Salt contribution to the flexibility of single-stranded nucleic acid of finite length*. Biopolymers, 2013. **99**(6): p. 370-381.